Shreyas Gaikwad Shane McQuarrie Caleb Phillips Bassel Saleh

In this problem, we revisit the sphere drop of problem 2, but with a different fluid. The same graduated cylinder is used as in problem 2, but instead of silicone oil we have a solution of a polymer (carbopol) in water (0.125% by weight). Three steel spheres of different diameters and one teflon sphere were dropped. For each sphere, the vertical location y of the sphere relative to the top of the fluid (positive down) was measured at constant intervals in time. The data are provided in Table 1 and Figure 1.

	Material	Nominal Diameter (in)	Measured Diameter (mm)
sphere 1	steel	0.2500	6.35
sphere 2	steel	0.3750	9.53
sphere 3	steel	0.1875	4.76
sphere 4	teflon	0.5000	12.70

Table 1: Specifications for the four spheres used in the experiment.

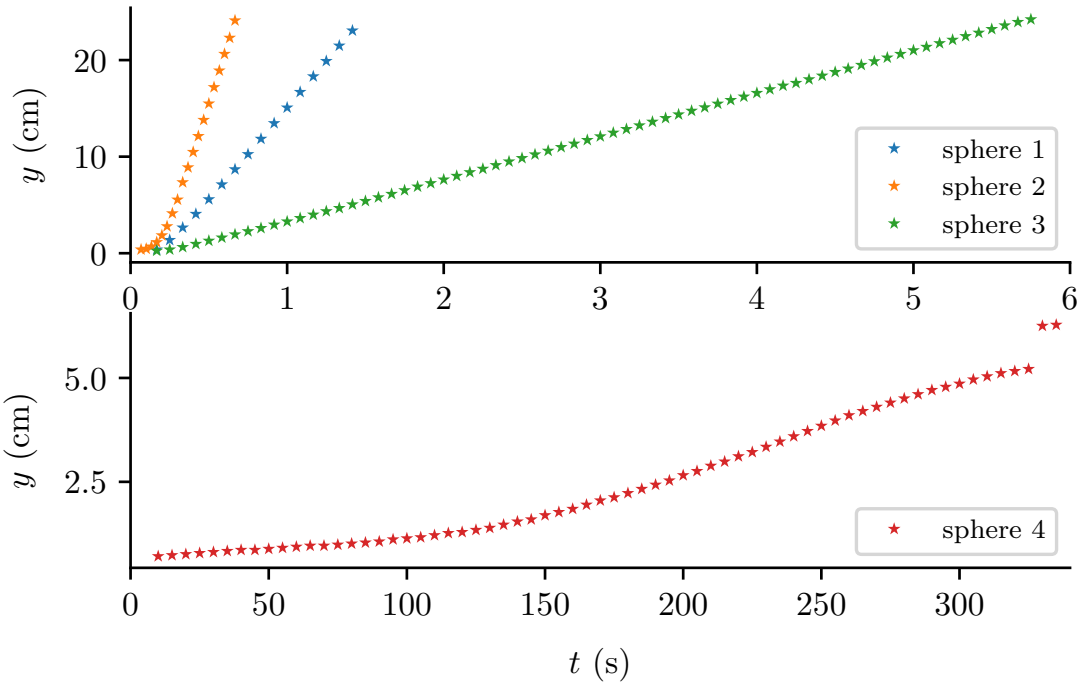

Figure 1: Raw data for each sphere, grouped by material: steel on top, teflon on bottom. Note that the last two measurements for the teflon sphere are highly irregular (this is likely due to a typo in the data); we will simply discard these points for our analysis.

The diameter of each sphere was measured, but they were not weighed. However, these spheres are made of the same steel and the same teflon materials as the spheres used in Problem 2.

It is proposed that Stokes flow with a Newtonian viscous stress model is a good model for this system. We will use Brenner's solution for a sphere moving along the axis of a cylinder,

$$F_d = \frac{3\pi\mu dV}{1 - [2.1044 - 0.6977\beta^2 + \mathcal{O}(\beta^4)]\alpha + \mathcal{O}(\alpha^3)}, \tag{1}$$

to calibrate and validate this model.

1. There are several ways to approach estimating the velocity with uncertainty. One is to identify a time window for each sphere over which the velocity is approximately constant, and then use the time/distance data in that time window to infer the velocity from the following linear model:

$$y = Vt + y_0 + \varepsilon \tag{2}$$

Where V is the velocity, y_0 is the offset (position at $t = 0$), and ε is the observation error. We assume that ε follows a Gaussian distribution with zero mean and some variance σ^2, i.e., $\varepsilon \sim \mathcal{N}(0, \sigma^2)$ (this is a common assumption for observation noise). The important uncertainties in (2) are the uncertainties in the offset y_0, data uncertainty due to observation error ε (encapsulated by σ), and the uncertainty in the value of terminal velocity V. For prior information, we select

$$y_0 \sim \mathcal{U}(-25\text{cm}, 25\text{cm}), \qquad \sigma \sim \mathcal{U}(0, 25\text{cm}), \qquad V \sim \mathcal{U}(0, gT),$$

where $T = \max_k\{t_k\}$ is the maximum observation time for a given sphere, i.e., gT is the maximum velocity a sphere would have after falling for that long it were falling in a vacuum. We take 25 cm as an upper bound for the height of the cylinder.

For a sphere with data $\mathbf{t} = \begin{bmatrix} t_1 & \cdots & t_n \end{bmatrix}^\mathsf{T}$ and $\mathbf{y} = \begin{bmatrix} y_1 & \cdots & y_n \end{bmatrix}^\mathsf{T}$, we have the following Bayesian parameter inference problem:

$$\begin{aligned} p(V, y_0, \sigma|\mathbf{t}, \mathbf{y}, X) &\propto p(\mathbf{t}, \mathbf{y}|V, y_0, \sigma, X)p(V, y_0, \sigma|X) \\ &\propto p(\mathbf{t}, \mathbf{y}|V, y_0, \sigma, X)p(V|X)p(y_0|X)p(\sigma|X) \qquad \text{(independence)} \\ &= \left(\prod_{k=1}^{n} \Phi(y_k|Vt_k + y_0, \sigma^2)\right) F(V|0, g\max_k\{t_k\})F(y_0|-25, 25)F(\sigma|0, 25), \end{aligned}$$

where $\Phi(x|\mu, \sigma)$ is the p.d.f. of $\mathcal{N}(\mu, \sigma^2)$ evaluated at x and $F(x|a, b)$ is the p.d.f. of $\mathcal{U}(a, b)$ evaluated at x, i.e.,

$$\Phi(x|\mu, \sigma) = \frac{1}{\sigma\sqrt{2\pi}} e^{-\frac{1}{2}\left(\frac{x-\mu}{\sigma}\right)^2}, \qquad F(x|a, b) = \begin{cases} \frac{1}{a-b} & \text{if } a \le x \le b, \\ 0 & \text{else.} \end{cases}$$

We sample from the posterior $p(V, y_0, \sigma|\mathbf{t}, \mathbf{y}, X)$ with MCMC using the `emcee` package in Python. For each sphere, we select for the training data $\mathbf{t}$ and $\mathbf{y}$ the portions of the data that appear to be linear. In the case of the teflon sphere, we use the range of data that seems to be linear with the maximum slope (velocity). See Figure 2 and Table 2 for the MCMC results. Next, in each case, we select the mean posterior values of V, y_0, and σ, and plot the relationship (2) against the data. See Figure 3.

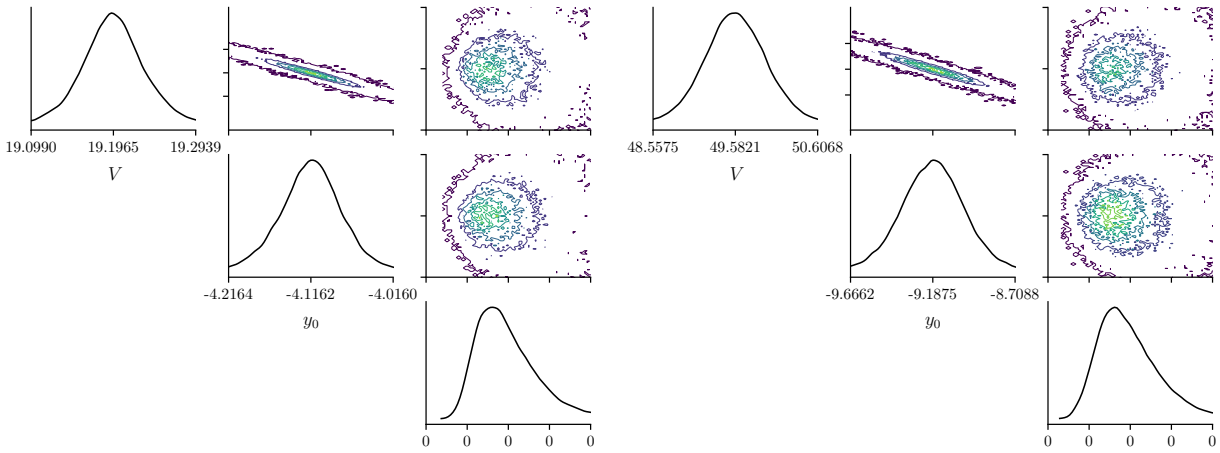

(a) Sphere 1.

(b) Sphere 2.

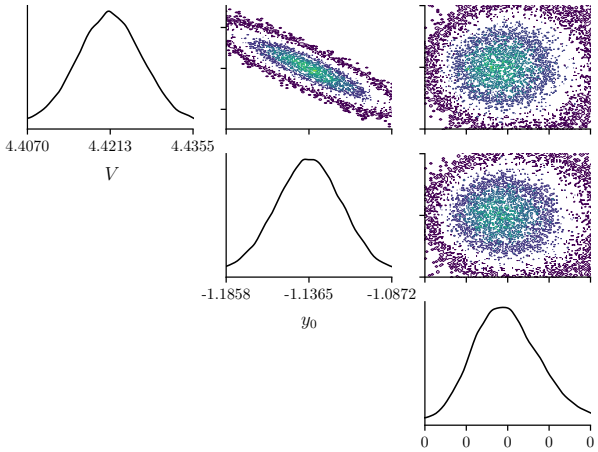

(c) Sphere 3.

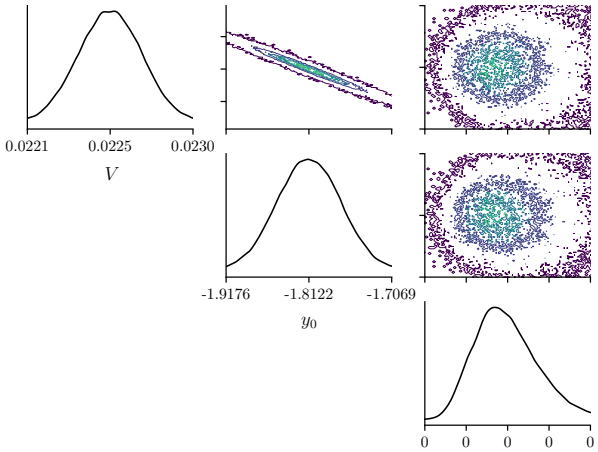

(d) Sphere 4.

Figure 2: Posterior distributions for V, y_0, and σ via MCMC.

	$\mathbb{E}[V] \pm \sqrt{\mathbb{V}\text{ar}[V]}$ cm/s	$\mathbb{E}[y_0] \pm \sqrt{\mathbb{V}\text{ar}[y_0]}$ cm	$\mathbb{E}[\sigma] \pm \sqrt{\mathbb{V}\text{ar}[\sigma]}$ cm
sphere1	19.19646 ± 0.03898	-4.11619 ± 0.04007	0.03237 ± 0.00919
sphere2	49.58213 ± 0.40985	-9.18753 ± 0.19148	0.19935 ± 0.04768
sphere3	4.42127 ± 0.00569	-1.13654 ± 0.01972	0.07164 ± 0.00657
sphere4	0.02250 ± 0.00018	-1.81224 ± 0.04215	0.04025 ± 0.00589

Table 2: Means and standard deviations statistics for each MCMC posterior.

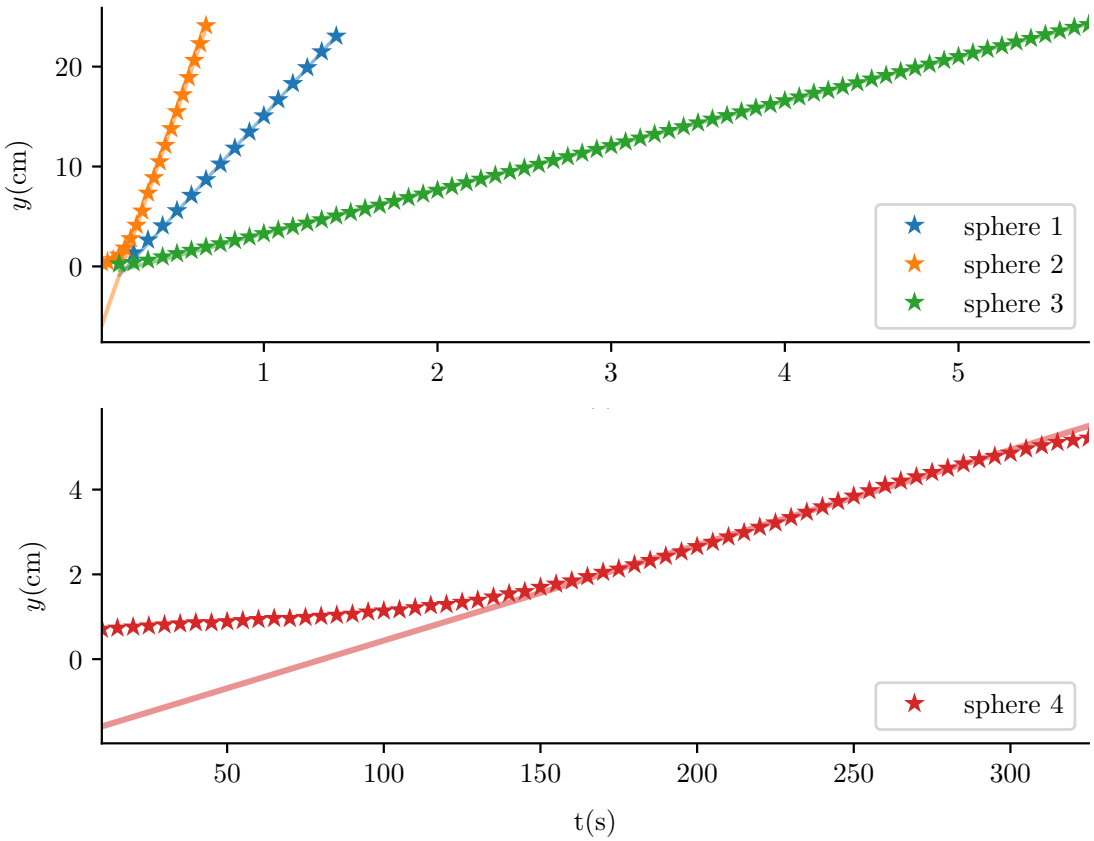

Figure 3: Data for each sphere and a consistency check of (2). The lines are actually shaded regions of $Vt + y_0 \pm \sigma$ but σ is relatively small in each case.

From Figure 3, we get the results that we expect: the linear model (2) with appropriate parameters match the training data very well, which validates our assumptions that the steel spheres do reach and maintain a constant terminal velocity (at least, over the time intervals that were used in the training). While the steel spheres quickly accelerate to their terminal velocities, it takes about two minutes for the teflon to reach what appears to be terminal velocity, and after about five minutes the velocity appears to decrease slightly. This should cause us to be a little concerned about the assumption of terminal velocity for the teflon sphere, but so far the steel spheres appear to have behaved well for our problem.

2. Using Brenner's solution along with $\beta = 0$, and since we are working in a window where the velocity is approximately constant, balancing the forces of drag, buoyancy, and gravity leads us to the Stokes' model

$$\mu = \frac{g\left(1 - 2.1044\frac{d}{D}\right)}{3\pi V d}\left(m - \frac{\pi\rho_f d^3}{6}\right), \tag{3}$$

where $g = 9.8\text{m/s}^2$ is the gravitational constant, $D = 68.15\text{mm}$ is the diameter of the cylinder, and ρ_f is the density of the fluid. We ignore uncertainties in g and D.

We can compute the density of ρ_f from the background information: we have a 0.125% polymer solution in water, which is 1.25 kg of solute in 1 m^3 water (the water itself weighs 1000 kg here). Therefore,

$$\rho_f = 1001.25 \, \frac{\text{kg}}{\text{m}^3} = 1.00125 \, \frac{\text{g}}{\text{cm}^3}.$$

As with g and D, we do not account for uncertainties in ρ_f. Since we don't have the mass data, we model the mass of the spheres as $m = \rho_s \pi d^3/6$, where ρ_s is the density of the sphere. Following group problem 2, we use densities $\rho_{\text{teflon}} \approx 2145\text{kg/m}^3 = 2.145\text{g/cm}^3$ and $\rho_{\text{steel}} \approx 7815\text{kg/m}^3 = 7.815\text{g/cm}^3$. Substituting for m in (3), we obtain

$$\begin{aligned} \mu = \frac{g\left(1 - 2.1044\frac{d}{D}\right)}{3\pi V d}\left(m - \frac{\pi \rho_f d^3}{6}\right) &= \frac{g\left(1 - 2.1044\frac{d}{D}\right)}{3\pi V d}\left(\frac{\rho_s \pi d^3}{6} - \frac{\pi \rho_f d^3}{6}\right) \\ &= \frac{g d^2(\rho_s - \rho_f)}{18V}\left(1 - 2.1044\frac{d}{D}\right), \end{aligned} \tag{4}$$

and, rearranging the terms,

$$V(\mu, d) = \frac{g d^2(\rho_s - \rho_f)}{18\mu}\left(1 - 2.1044\frac{d}{D}\right). \tag{5}$$

Substitute this expression for V into (2) yields

$$y = \frac{g d^2(\rho_s - \rho_f)}{18\mu}\left(1 - 2.1044\frac{d}{D}\right) t + y_0 + \varepsilon. \tag{6}$$

We now repeat the Bayesian inference from part 1, but this time we infer μ instead of V:

$$\begin{aligned} p(\mu, y_0, \sigma | \mathbf{t}, \mathbf{y}, X) &\propto p(\mathbf{t}, \mathbf{y} | \mu, y_0, \sigma, X) p(\mu, y_0, \sigma | X) \\ &\propto p(\mathbf{t}, \mathbf{y} | V, y_0, \sigma, X) p(\mu | X) p(y_0 | X) p(\sigma | X) \qquad \text{(independence)} \\ &= \left(\prod_{k=1}^{n} \Phi\left(y_k | V(\mu, d_k) t_k + y_0, \sigma^2\right)\right) F(\mu | 0, \mu_{\max}) F(y_0 | -25, 25) F(\sigma | 0, 25), \end{aligned}$$

where $V(\mu, d)$ is given by (5). For the prior of this viscosity, we set $\mu \sim \mathcal{U}(0, \mu_{\max})$ since viscosity is a positive quantity, and we choose $\mu_{\max} = 50\text{g/cm} \cdot \text{s}$ based on the background information that the solution is carbopol in water (this is an exaggerated upper bound). We use the same calibration data here as with the calibration done in part 1 except that we exclude the data for the teflon sphere, and we use all of the data in a single calibration instead of doing one calibration per sphere.

To get a reasonable initial guess for μ to be used by the MCMC sampler, we use (4) with the measured diameters in Table 1 and the mean values of V in Table 2, which yields a guess μ for each sphere: $\mu_1 \approx 7.78515$, $\mu_2 \approx 6.78211$, and $\mu_3 \approx 19.00366$ (in units of g·s/cm). The discrepancy between these is concerning, but we attempt the MCMC calibration anyway.

Figure 4 shows the results when the model is calibrated using training data from all three steel spheres; Figure 5 shows posterior marginal distributions for μ and y_0 when the calibration data is taken from each of the spheres individually, and when the from the data from all three steel spheres is combined; and Table 3 shows the statistics of each posterior.

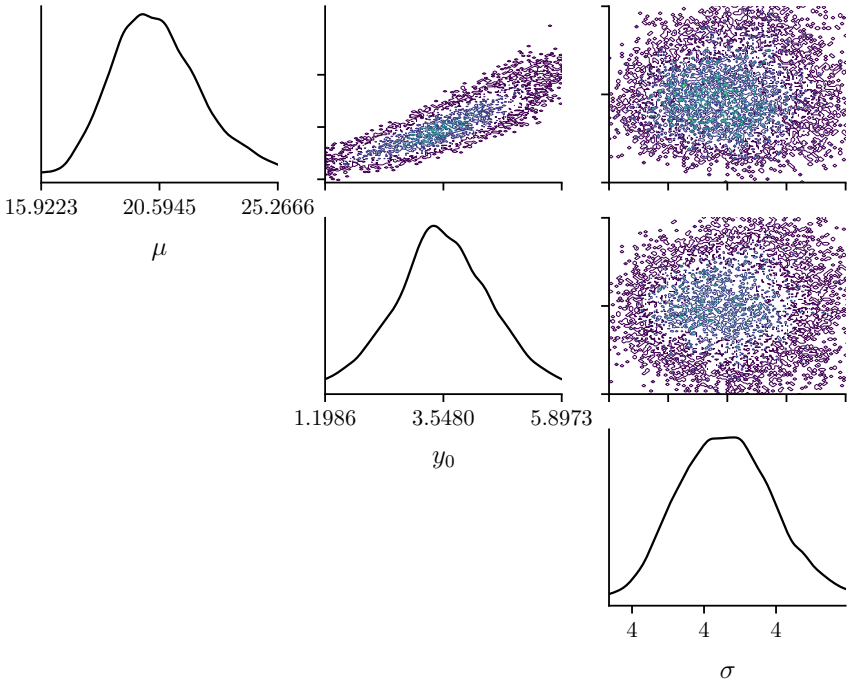

Figure 4: Posterior distributions for μ, y_0, and σ via MCMC.

The marginal posterior for μ in Figure 4 gives a larger estimate than the initial guesses for each sphere; indeed, it appears at first glance that the data from sphere 3 may be swamping the data from spheres 1 and 2, since $\mathbb{E}[\mu] \approx 20.5945$ is near the rough estimate $\mu_1 \approx 19.0037$. However, the spread of the distribution for μ is quite large, and the marginal posterior distributions for y_0 and σ are quite different than the corresponding distributions in the velocity calibration reported in Figure 2. In order to try to get a better result, we perform this MCMC calibration again using only data from sphere 1, again using only data from sphere 2, and again with only data from sphere 3. In Figure 5, we plot the marginal posteriors of μ and y_0 for each experiment. Table 3 details the statistics. There is a clear lack of consistency across these different inference experiments, and the only set of results that appears confident (low-variance posteriors and a small expected value of σ) is the trial where we only use data from sphere 3 to calibrate (6).

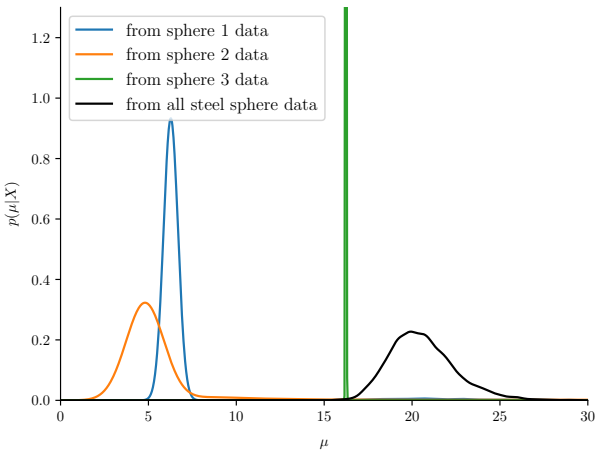

(a) Posterior distributions for μ via MCMC from various calibration data.

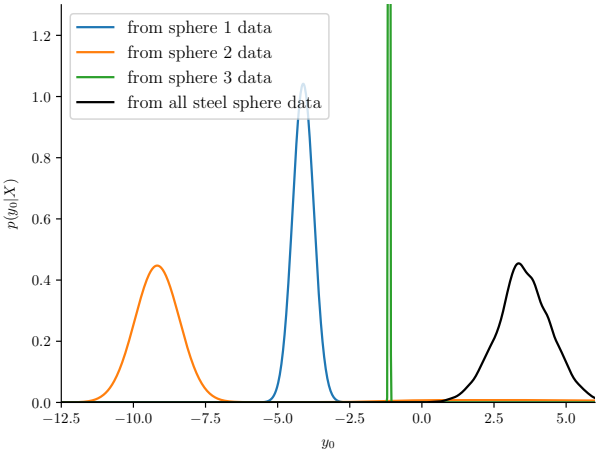

(b) Posterior distributions for y_0 via MCMC from various calibration data.

Figure 5: Bad news.

	$\mathbb{E}[\mu] \pm \sqrt{\mathbb{V}\text{ar}[\mu]}$ g/cm·s	$\mathbb{E}[y_0] \pm \sqrt{\mathbb{V}\text{ar}[y_0]}$ cm	$\mathbb{E}[\sigma] \pm \sqrt{\mathbb{V}\text{ar}[\sigma]}$ cm
all steel spheres	20.05420 ± 1.71460	3.52721 ± 0.87755	4.14500 ± 0.31603
sphere1	6.91442 ± 3.57466	-3.56154 ± 2.69637	0.10783 ± 0.36359
sphere2	6.03822 ± 5.72269	-8.15991 ± 4.08431	0.49119 ± 1.21272
sphere3	16.23340 ± 0.02093	-1.13643 ± 0.01983	0.07152 ± 0.00642

Table 3: Means and standard deviations statistics of each MCMC posterior for the calibration in Figures 4–5.

3. It is clear already from Figure 5 that the steel sphere data is not consistent with the calibrated Stokes flow Newtonian viscous model, but we attempt a posterior predictive check of sorts anyway (in general, a posterior predictive check is really only useful in situations where the model may or may not be valid; in our case, it already seems that the model is invalid, so there is really no point in doing a complete posterior predictive check). First, we take the average values of μ, y_0, and σ when the model had been calibrated from all steel sphere data ($\mu \approx 20.05420$, $y_0 \approx 3.52721$ and $\sigma \approx 4.145$), and use them in (6) together with the data for d and t to predict y (this is similar to what we did in Figure 3). The results, in the upper plot of Figure 6, are terrible. To get a better result, we use the average values of μ, y_0 and σ from the calibration that only uses sphere 3 data ($\mu \approx 16.23340$, $y_0 \approx -1.13643$, and $\sigma \approx 0.07152$), and repeat the process, only predicting y for the sphere 3 data in d and t. These results, in the lower plot of Figure 6, are much better. This is to be expected, because the MCMC posteriors that come from using only data from sphere 3 are tight. However, this success does not validate the Stokes flow model; rather, it gives us confidence that the MCMC procedure worked correctly.

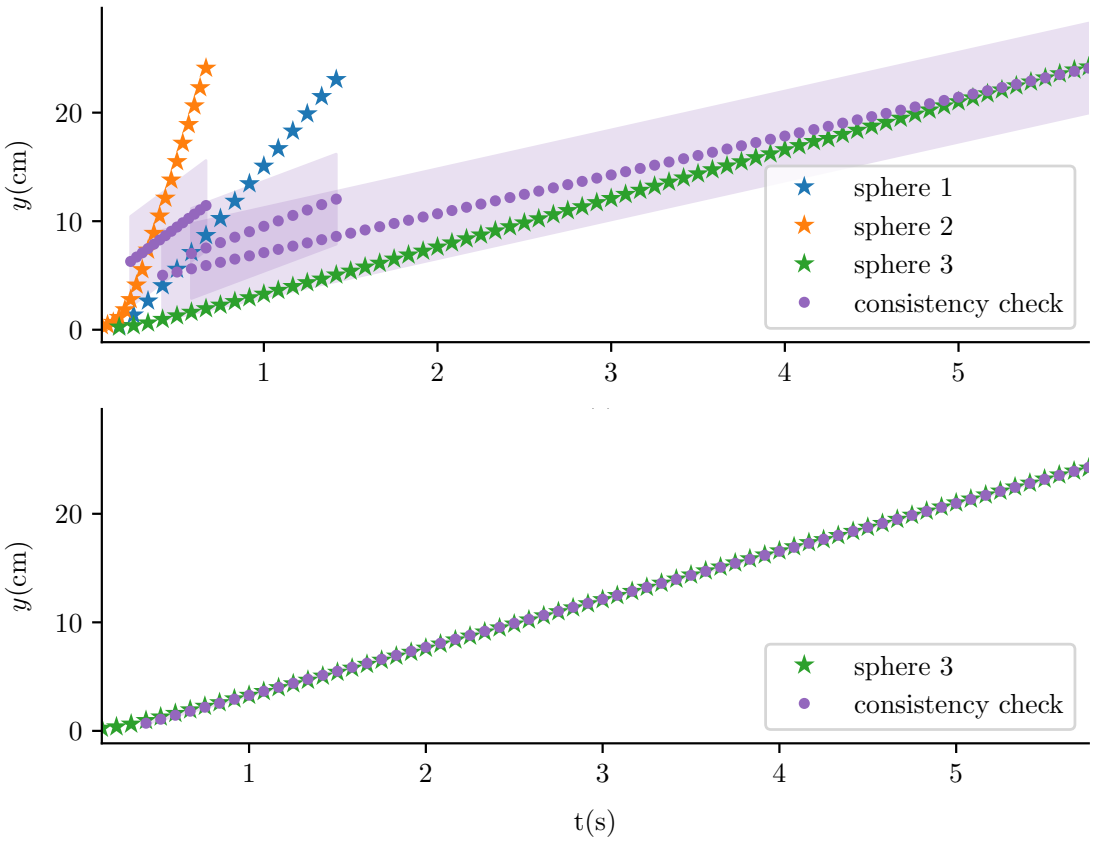

Figure 6: Data for each sphere and a consistency check of (6). The purple dots $\hat{y}$ is calculated from (6) given some μ y_0, and σ, and the shaded purple regions represent $\hat{y} \pm \sigma$. The upper plot uses μ, y_0, and σ from the calibration with all steel sphere data; the lower plot uses μ, y_0, and σ from the calibration with only sphere 3 data.

4. As an even more stringent validation test, we use the average values of μ, y_0, and σ obtained by calibrating with just the data from sphere 3 and try to use (6) to predict the data for the teflon sphere is consistent with the model. This is a more stringent test than before because we trying to match data that lies outside of our calibration training set. Unfortunately, the result, shown in Figure 7, is terrible. In other words, this particular calibration is consistent with the calibration data itself, but it does not work well for the prediction case at all.

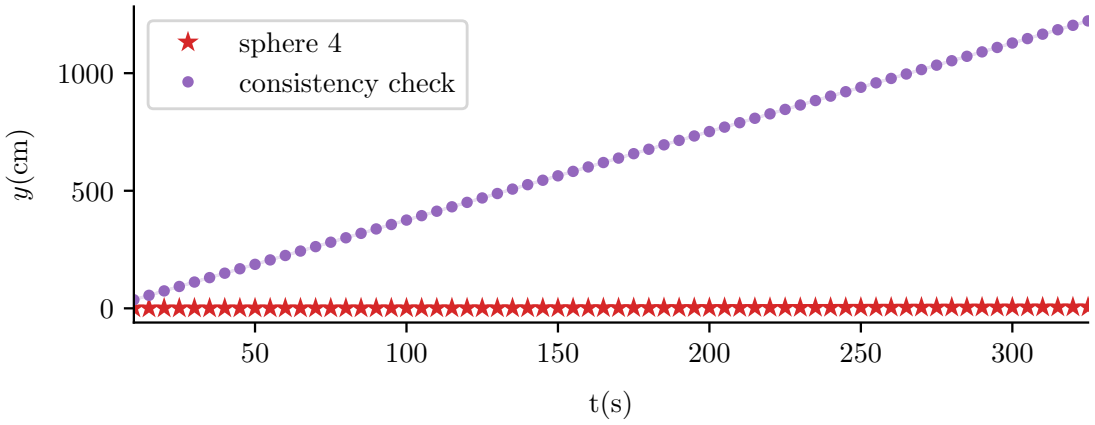

Figure 7: Data for sphere 4 and a consistency check of (6).

5. The data from the teflon sphere is not consistent with the calibrated model, and the data from the individual steel spheres also appear to be inconsistent with each other. This raises the following question: is the Stokes' law model even applicable in our situation?

   Stokes' law assumes a laminar flow (very low Reynolds Number regime, i.e., Re $\ll 1$) in a *Newtonian fluid*, spherical particles, homogeneous (uniform in composition) material, smooth surfaces, and that the particles do not interfere with each other. By using the guess $\mu \approx 16.23340$ (from the calibration with only sphere 3 data) and the average values of the velocity V calculated in part 1 (see Table 2), we compute the Reynolds number Re $= \rho_f V d/\mu$ for each spheres 1–4 to be 0.75183, 2.91382 , 0.12980, and 0.00176, respectively. The high values of Re for spheres 1 and 2 (especially 2) are a big problem for the laminar flow assumption.

   Furthermore, it turns out that a carbopol solution is *NOT* a Newtonian fluid. This means another of the key assumptions for Stokes flow is invalid, but this is a problem that is independent of the spheres (which could explain why the teflon sphere, though it induces a low Re, does not maintain its terminal velocity). We also have no information about the homogeneity, smoothness, and "sphericality" of the spheres. This final aspect could be particularly troublesome, but we have no way of reducing such uncertainty.

Appendix A: Code

See our Google Colab notebook:
`https://colab.research.google.com/drive/1fWsNL1ycErMoulZbV_YjCSrS76i9ACvW`.

Appendix B: A Quote